# On the Evaluation of Linear and Non-Linear Models Using DNS Data of Turbulent Channel Flows

**Hasna BenSaid**
bs_hasna2004@yahoo.fr
Faculté des sciences de Gafsa
Campus Universitaire Sidi Ahmed Zarroug
2112 Gafsa, Tunisie

**Gilmar Mompean**
gilmar.mompean@polytech-lille.fr
Université Lille I
LML, UMR CNRS 8107
Boulevard P. Langevin
F-59655 Villeneuve d'Ascq, France

**Hassane Naji**
hassane.naji@univ-artois.fr
Université d'Artois/FSA/LGCgE EA 4515
Université Lille Nord de France
Technoparc Futura
F-62400 Béthune, France

*In this paper, a priori and a posteriori analyses of algebraic linear and non-linear models are carried out in order to compare their ability to predict near wall turbulent flows. Tests were done using data from a direct numerical simulation (DNS) of a plane channel flow for three Reynolds numbers, based on the friction velocity, $Re_\tau = 180$, $Re_\tau = 395$ and $Re_\tau = 590$. These models include the linear standard $k-\varepsilon$ model, the linear $v^2-f$ (Manceau et al., 2002) and the non-linear model of Shih (Shih et al., 1995). The results obtained are then compared with the DNS data of Moser et al. (1999). The comparisons are shown for the mean velocity profile, components of the Reynolds stress tensor, the turbulent kinetic energy ($k$), and the dissipation rate ($\varepsilon$). The results suggest that the $v^2-f$ is an efficient model to capture the turbulent shear stress component of the Reynolds stress near wall flows. However, it is unable to predict correctly the level of anisotropy between normal components of the Reynolds stress tensor. Furthermore, it is shown that the presence of non-linear terms in a turbulent model improves the ability to predict the anisotropy*

***Keywords:*** *Near-wall turbulence, $\overline{v^2}-f$ model, non-linear model, elliptic relaxation model*

## Introduction

In the field of turbulence modeling, there is a whole hierarchy of models to close the Reynolds stress tensor, when the Reynolds averaged Navier-Stokes equations (RANS) approach is used. One of the difficulties the modeler faces when using computational fluid dynamics (CFD) numerical codes is on how to choose the best turbulent model to solve his problem. These models range from zero up to six differential equations. For models having more than two equations, they are frequently based on the turbulent kinetic energy ($k$) and its dissipation rate ($\varepsilon$). In these models, an eddy viscosity is also introduced in order to close the Reynolds stress tensor. Despite the efforts, it is generally agreed that, presently, there is no dominant turbulent model that can be universally used for complex flows. The pursuit of an improved model, based on the RANS approach, is most likely to continue. The industrial applications of CFD using these models are numerous: prediction of turbulence level for aerodynamics and hydrodynamics fields, forced convection, fluid-structure interaction, etc. Hines et al. (2009) studied numerically a turbulent flow over a square cylinder with prescribed and autonomous motions using a turbulent model to reduce the excessive production of turbulent kinetic energy in the stagnation region in front of the square cylinder. They were interested in the lock-in phenomenon where the effects of the forced oscillations dominate the flow. Goldberg el al. (2009) tested the performance of a model, based on transport equations of $k$, $\varepsilon$ and an undamped eddy viscosity for two aerodynamics flow cases. They found that the model is shown to revert to the $k-\varepsilon$ model in near wall flow regions.

Durbin (1991, 1993) shows that these models are not efficient enough to predict turbulent flows near wall, especially because they need a boundary correction function $f_\mu$, since they are unable to predict the near-wall zone. It should be noted that several relationships have been proposed for a damping function. To overcome these deficiencies, Durbin proposes a model based on the normal component of the Reynolds stress, so called $\overline{v^2}-f$ model, in which the correction is implemented via an elliptic differential equation, suggesting a new scale for the velocity to capture the anisotropy in the near wall region. In other words, a linear relation between the Reynolds stress and the deformation rate tensor is postulated throughout an eddy viscosity based on the wall-normal component of the Reynolds tensor ($\overline{v^2}$).

The papers of Mompean et al. (1996), and of Naji et al. (2004), show the behaviour of some nonlinear models when predicting the turbulent flow in a square duct. The results clearly show that the presence of non-linear terms is important to capture the anisotropy of the turbulent stress, in the case of the square duct, responsible for the secondary flow. Moosavi and Grandjalikhan Nassab (2008) have conducted a numerical study on the turbulent forced convection over a single inclined forward step in a duct also using non-linear $k-\varepsilon$ model. They found that step length and inclination angle have important effects on the hydrodynamic behaviour of the flow.

More recently, Thompson et al. (2010) showed how the eddy viscosity depends on the kinematic tensors for plan channel and square duct flows. It is clearly proved that using only the Boussinesq eddy viscosity is not sufficient to predict the anisotropy of the Reynolds stress tensor. For this, the inclusion of non-linear terms seems necessary.

Another kind of approach is used in the paper of Qiu et al. (2011), presenting a new model based on the analogy between laminar flows of non-Newtonian fluids and turbulent flows of Newtonian fluids. This model is based on the first and second normal stress difference, normally used in viscoelastic (non-Newtonian) fluids. This model is very promising since it does not use the $k-\varepsilon$ turbulent scales, making the calculation less expensive.

The main objective of this work is to study the models by *a priori* and *a posteriori* tests, using the DNS data of Moser et al. (1999). The methodology of the *a priori* and *a posteriori* tests is described in the section concerning the numerical study.

**Paper received 12 April 2011. Paper accepted 14 February 2012**
**Technical Editor: Francisco Cunha**

In this paper, we consider three turbulent models: ***i***) the linear standard $k-\varepsilon$ model, ***ii***) the linear $\overline{v^2}-f$ (Manceau et al., 2002) and ***iii***) the non-linear model of Shih et al. (1995). The prediction capabilities of these three models are evaluated by comparison with the available DNS data (see Moser et al. (1999)).

The results of the tests are presented for a plan channel turbulent flow at different Reynolds numbers and will be of interest to the reader working with turbulence modeling. It is also useful to improve turbulent models and help to decide how to choose an appropriate turbulent model for numerical simulations using Reynolds Averaged Navier-Stokes equations. These considerations can depend on the kind of flow being modeled, i.e. predominant shear flows like boundary layers, and/or flows presenting secondary flows where the anisotropy between the Reynolds stress normal components is important.

This paper is organized as follows. The next section presents the numerical study and the details of the tested models. The section Results and Discussion presents and comments the principal results obtained in this work. Conclusions are drawn in the final section.

## Nomenclature

| | |
|---|---|
| $C_1, C_2, C_\eta, C_L, C_T$ | *= f-equation coefficients* |
| $C_{\varepsilon 1}, C_{\varepsilon 2}$ | *= dissipation equation coefficients* |
| $C_\mu$ | *= turbulent viscosity constant* |
| $f$ | *= source term of the* $\overline{v^2}-$ *equation* |
| $f_\mu$ | *= damping wall function* |
| $k$ | *= turbulent kinetic energy (=* $\overline{u_i u_i}/2$*)* |
| $k^+$ | *= dimensionless turbulent kinetic energy* |
| $L$ | *= turbulent length scale* |
| $P_k$ | *= turbulent production (=* $2\nu_t S_{ij} S_{ij}$*)* |
| $Re_\tau$ | *= Reynolds number based on friction velocity (*$Re_\tau = u_\tau \delta/\nu$*)* |
| $S_{ij}$ | *= mean flow strain rate tensor* |
| $S^*$ | *= strain rate magnitude* |
| $T$ | *= turbulent time scale* |
| $\overline{u_i u_j}$ | *= Reynolds stress tensor* |
| $\overline{uu}, \overline{vv}, \overline{ww}$ | *= Reynolds normal stresses* |
| $u_\tau$ | *= friction velocity (=* $\sqrt{\tau_w/\rho}$*)* |
| $U, V, W$ | *= mean streamwise, vertical and spanwise velocity, respectively* |
| $u, v, w$ | *= fluctuating velocity components* |
| $x, y, z$ | *= streamwise, normal and spanwise coordinate directions* |
| $y^+$ | *= dimensionless normal distance from wall (=* $yu_\tau/\nu$*)* |

**Greek Symbols**

| | |
|---|---|
| $\delta$ | *= channel half-width* |
| $\delta_{ij}$ | *= Kronecker delta* |
| $\varepsilon$ | *= turbulent dissipation rate* |
| $\varepsilon^+$ | *= dimensionless turbulent dissipation rate* |
| $\nu$ | *= kinematic molecular viscosity* |
| $\nu_t$ | *= turbulent viscosity* |
| $\Omega_{ij}$ | *= mean flow rotation rate tensor* |
| $\Omega^*$ | *= rotation rate magnitude* |
| $\sigma_{(k,\varepsilon)}$ | *= appropriate turbulent Prandtl numbers* |
| $\tau_w$ | *= shear stress at the wall* |

**Superscripts**

| | |
|---|---|
| $^+$ | *= quantity normalized by* $u_\tau$ *and* $\nu$*.* |

## Numerical Study

### *A priori* study

The methodology of an *a priori* test of turbulence models consists in using mean field turbulent values coming from Direct Numerical Simulation (DNS) of the Navier-Stokes equations. The mean velocity components ($U$, $V$ and $W$), the turbulent kinetic energy ($k$) and its dissipation rate ($\varepsilon$) obtained through the DNS computations are supplied explicitly in the equations of the turbulence models providing predictions for Reynolds stress components. In this way, the model gives explicitly the values of the Reynolds stress components in function of the mean values computed by the DNS. These predictions are then compared with the Reynolds stress components evaluated directly from the DNS. Figure 1 illustrates the procedure of the *a priori* test. Details of this procedure can be found in Mompean et al. (1996). The results of the *a priori* analysis will show how the model, through its algebraic expression, is compatible with the Navier-Stokes equations.

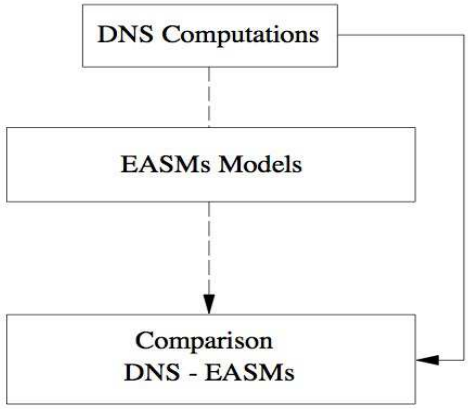


**Figure 1. The *a priori* test.**

### DNS data

The DNS data used here are those of Moser et al. (1999). This work concerns a fully developed plane turbulent channel flow, which was carried out for three different Reynolds numbers, namely $Re_\tau = 180$, $Re_\tau = 395$ and $Re_\tau = 590$ where $Re_\tau = u_\tau \delta/\nu$; $u_\tau$ and $\delta$ being the friction velocity and the channel half-width, respectively.

Below are described the characteristics of the numerical simulations done by Moser et al. (1999) using a DNS code. The numerical method uses a Chebychev-tau formulation in the wall–normal direction ($y$) and a Fourier representation in the horizontal directions. A low-storage third-order Runga–Kutta time discretization is used for the nonlinear terms. Periodic boundary conditions are applied in the streamwise ($x$) and spanwise ($z$) directions, and the pressure gradient that drives the flow was adjusted dynamically to maintain a constant mass flux through the channel. The periodic domain sizes were selected so that the two-point correlations in the streamwise and spanwise directions would be essentially zero at maximum separation (half the domain size), while the number of Fourier/Chebychev modes (the resolution) was selected so that the energy spectra would be sufficiently small at large wave numbers. For the three different Reynolds numbers cases, there are 13 or more Chebychev grid points below $y^+ = 10$,

showing the boundary layer is well resolved. More details can be found in the paper of Moser et al. (1999).

**Governing equations and turbulence models for the RANS calculations**

In order to model the problem of an incompressible flow in a turbulent regime, using the Reynolds Averaged Navier-Stokes equations, the mass and momentum conservation equations are used and coupled with a turbulent model to obtain the Reynolds stress components ( $\overline{u_i u_j}$ ).

**The $k-\varepsilon$ model**

The $k-\varepsilon$ model retained in this paper is the classical one, which is based on the Boussinesq approximation to model the Reynolds stresses:

$$\overline{u_i u_j} = \frac{2}{3}k\delta_{ij} - 2\nu_t S_{ij} \tag{1}$$

where $\delta_{ij}$ is the Kronecker tensor , $S_{ij} = (U_{i,j} + U_{j,i})/2$ is the mean rate of the deformation tensor, $U_{i,j}$ is the velocity gradient and $U_{j,i}$ is its transpose. $\nu_t = C_\mu k^2/\varepsilon$ is the so-called turbulent eddy viscosity, where $C_\mu = 0.09$, $k$ is the turbulent kinetic energy and $\varepsilon$ is its dissipation rate. These two scales ($k$ and $\varepsilon$) are obtained from two differential equations, and are used to evaluate the eddy viscosity. These equations are derived from the Navier-Stokes equations using the Reynolds decomposition for the instantaneous field (velocity and pressure). In this decomposition, the fields are decomposed in mean and fluctuating parts and replaced in the mass and momentum conservation equations. The two differential equations, for $k$ and $\varepsilon$, are presented in the next section, respectively Eqs. (4) and (5).

For the near-wall region, a damping function $f_\mu$ is used in order to improve the prediction in the vicinity of the wall. Therefore, the turbulent eddy viscosity is modified as follows:

$$\nu_t = C_\mu f_\mu k^2/\varepsilon \tag{2}$$

In this work, we have chosen the following (see Chien, 1982) $f_\mu$ expression:

$$f_\mu = 1. - \exp(-0.0115 y^+) \tag{3}$$

where $y^+$ is the dimensionless wall distance based on the friction velocity $u_\tau$ and the kinematic viscosity $\nu$.

**The $\overline{v^2} - f$ model**

Hereafter, it is explained how the $\overline{v^2} - f$ model was obtained. The main idea of this model is to use a new turbulent scale to model the eddy viscosity. The scale concerning the normal stress component to the wall ( $\overline{v^2}$ ) is chosen because it can be used to express the anisotropy of the Reynolds stress normal components. Manceau et al. (2002) have shown how this choice can improve the predictions. The so-called $\overline{v^2} - f$ model consists of the transport equations for the turbulent kinetic energy, the isotropic dissipation rate, the $\overline{v^2}$ normal stress component.

$$\frac{Dk}{Dt} = \frac{\partial}{\partial x_j}\left(\left(\nu + \frac{\nu_t}{\sigma_k}\right)\frac{\partial k}{\partial x_j}\right) + P_k - \varepsilon \tag{4}$$

$$\frac{D\varepsilon}{Dt} = \frac{\partial}{\partial x_j}\left(\left(\nu + \frac{\nu_t}{\sigma_\varepsilon}\right)\frac{\partial \varepsilon}{\partial x_j}\right) + C_{\varepsilon 1}\frac{\varepsilon}{k}P_k - C_{\varepsilon 2}\frac{\varepsilon^2}{k} \tag{5}$$

$$\frac{D\overline{v^2}}{Dt} = \frac{\partial}{\partial x_j}\left(\left(\nu + \frac{\nu_t}{\sigma_k}\right)\frac{\partial \overline{v^2}}{\partial x_j}\right) + kf - \frac{\varepsilon}{k}\overline{v^2} \tag{6}$$

where $D/Dt$ is the material time derivative and $P_k = -\overline{u_i u_j}S_{ij}$ is the turbulent production term.

The commonly used set of constants is given as:

$$C_{\varepsilon 1} = 1.44\,,\ C_{\varepsilon 2} = 1.92\,,\ \sigma_k = 1.0\,,\ \sigma_\varepsilon = 1.3$$

It is useful to note that $f$ in Eq. (6) is the solution of an auxiliary elliptic equation, which is a modified Helmholtz equation, whose solution is close to an exponential decay as well as the wall is approached. Durbin (1991) introduced the elliptic relaxation approach within the framework of the linear eddy viscosity formulation. The $f-$ equation can be written as:

$$f - L^2\nabla^2 f = (C_1 - 1)\frac{\frac{2}{3} - \frac{\overline{v^2}}{k}}{\varepsilon T} + \frac{2}{3}C_2\frac{P_k}{k} \tag{7}$$

where the time scale $T$ is $k/\varepsilon$, which is bounded near the wall by the Kolmogorov scale $\sqrt{\nu/\varepsilon}$. The length scale is formulated by analogy to the time scale $T$. Then, the two scales are respectively given by:

$$T = \max\left(\frac{k}{\varepsilon}, C_T\sqrt{\frac{k}{\varepsilon}}\right) \tag{8}$$

$$L = C_L \max\left(\frac{k^{3/2}}{\varepsilon}, C_\eta\left(\frac{\nu^3}{\varepsilon}\right)^{1/4}\right) \tag{9}$$

with $C_1 = 1.8$ ; $C_2 = 0.6$ ; $C_T = 6.0$ ; $C_L = 0.38$ ; $C_\eta = 85.0$ .

Here, the turbulent eddy viscosity is expressed as:

$$\nu_t = C_\mu \overline{v^2} T \tag{10}$$

It should be noted that $\overline{v^2}$ is considered as an energy scale generalizing the wall-normal Reynolds stress component everywhere in the domain.

**The Shih model**

In this model, Shih et al. (1995) developed a general non-linear constitutive relation for the Reynolds tensor components,

starting from the Boussinesq equation. The expression of these components is:

$$\overline{u_i u_j} = \frac{2}{3}k\delta_{ij} - C_\mu \frac{k^2}{\varepsilon} 2S_{ij} + 2C_2 \frac{k^3}{\varepsilon^2}\left(-S_{ik}\Omega_{kj} + S_{kj}\Omega_{ik}\right) \quad (11)$$

The coefficients $C_\mu$ and $C_2$ are functions of the deformation and the rotation rates $S_{ij}$ and $C_2$:

$$C_\mu = \frac{1}{A_0 + A_S \dfrac{U^* k}{\varepsilon}}$$

$$C_2 = \frac{\sqrt{1 - 9C_\mu^2 (S^* k/\varepsilon)^2}}{\left(C_0 + 6\left(\dfrac{S^* k}{\varepsilon}\right)\left(\dfrac{\Omega^* k}{\varepsilon}\right)\right)}$$

$$U^* = \sqrt{S_{ij}S_{ij} + \Omega_{ij}\Omega_{ij}}\,,\ S^* = \sqrt{S_{ij}S_{ij}}\,,\ \Omega^* = \sqrt{\Omega_{ij}\Omega_{ij}}$$

$$A_0 = 6.5\,,\ A_S \in \left[\sqrt{6}/2, \sqrt{6}\right],\ C_0 = 1.0$$

with $\Omega_{ij} = \left(U_{i,j} - U_{j,i}\right)/2$.

## Results and Discussion

### *A priori* results

In this section, the results obtained with the *a priori* test for the three turbulent models are shown and commented. It should be noted that the wall normal Reynolds stress is taken from the DNS, and in conjunction with Eq. (10), we deduce the turbulent eddy viscosity. The dimensionless profiles of the normal stresses $\overline{uu}^+$, $\overline{vv}^+$, $\overline{ww}^+$ and shear stress $\overline{uv}^+$ ($\overline{u_i u_j}^+ = \overline{u_i u_j}/u_\tau^2; 1 \le i, j \le 3$) of the Reynolds stress tensor at $Re_\tau$=*180, 395* and *590* are shown from Fig. 2 to Fig. 5.

Figure 2 shows the profiles of normal stress for the streamwise direction obtained with the three turbulent models ($k-\varepsilon$, $\overline{v^2}-f$ and the Shih model) for three different Reynolds numbers. These results are compared with the DNS ones. We can see clearly that the Shih model gives the better agreement with the DNS, presenting a small over-prediction for the maximum value around $y^+$=*20*. The profiles predicted for the component $\overline{vv}^+$ are presented in Fig. 3. The Shih model gives the closest results with the DNS. For this component, the $k-\varepsilon$ and the $\overline{v^2}-f$ models over-predicted the values of about 300%. It should be mentioned that, when using the $\overline{v^2}-f$ model in *a posteriori* calculation, the $\overline{vv}^+$ Reynolds stress component is obtained from Eq. (6).

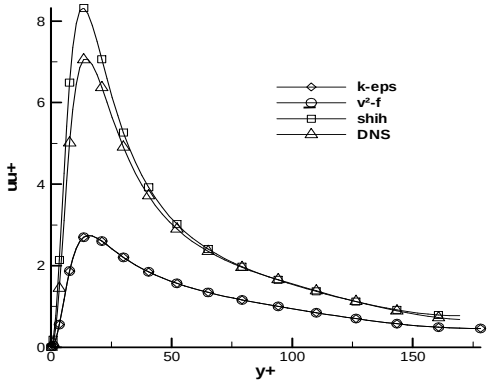


*(a)*

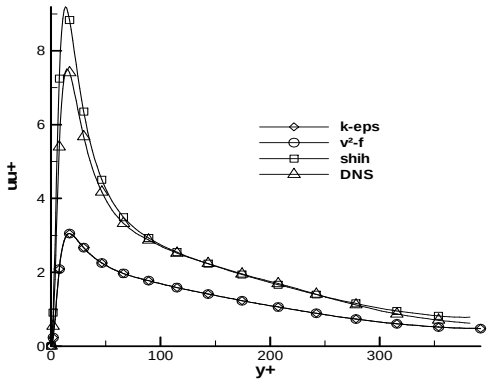


*(b)*

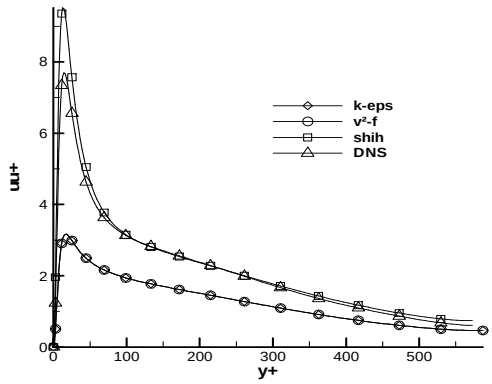


*(c)*

**Figure 2. Streamwise stress $\overline{uu}^+$. Comparison of models' predictions with DNS in a channel flow at (a) $Re_\tau = 180$, (b) $Re_\tau = 395$ and (c) $Re_\tau = 590$.**

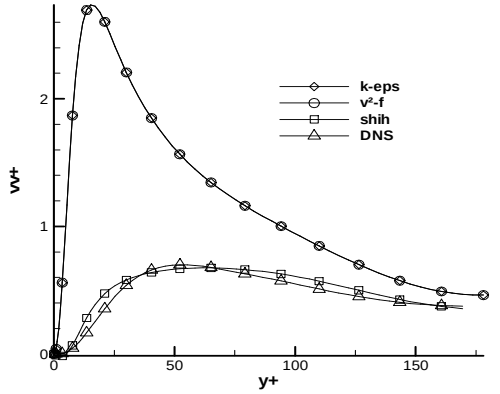


*(a)*

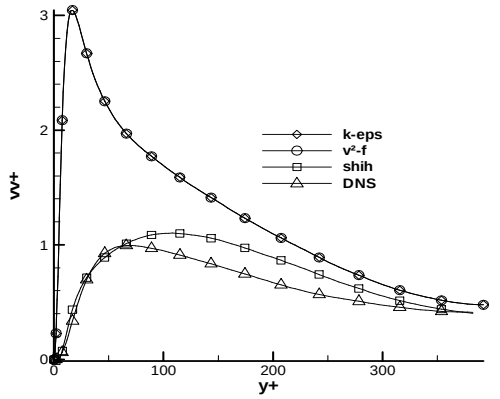


*(b)*

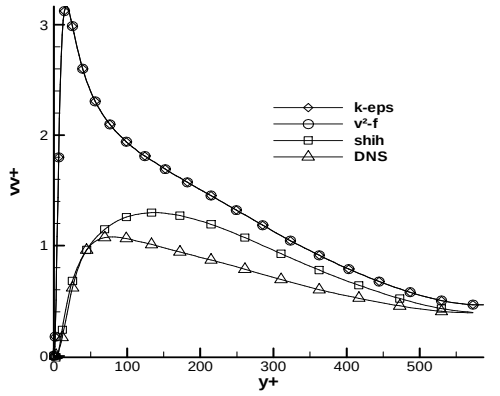


*(c)*

**Figure 3. wall-normal stress $\overline{vv}^+$. Comparison of models' predictions with DNS in a channel flow at (a) $Re_\tau = 180$, (b) $Re_\tau = 395$ and (c) $Re_\tau = 590$.**

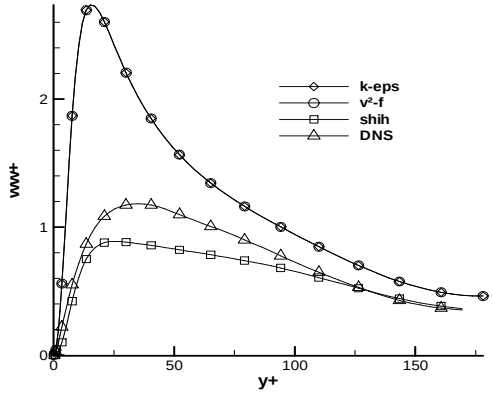


*(a)*

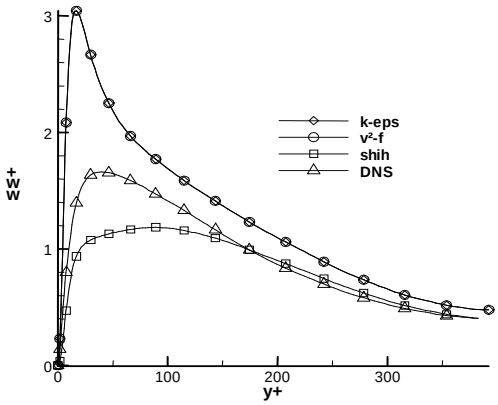


*(b)*

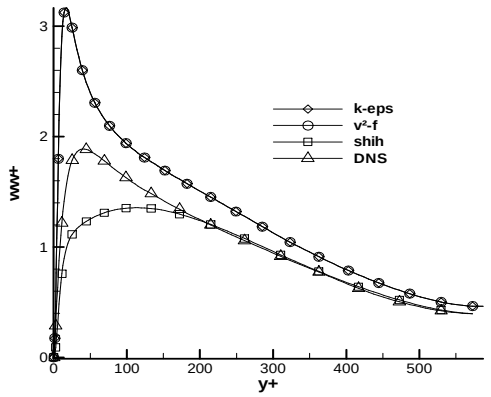


*(c)*

**Figure 4. Spanwise stress $\overline{ww}^+$. Comparison of models' predictions with DNS in a channel flow at (a) $Re_\tau = 180$, (b) $Re_\tau = 395$ and (c) $Re_\tau = 590$.**

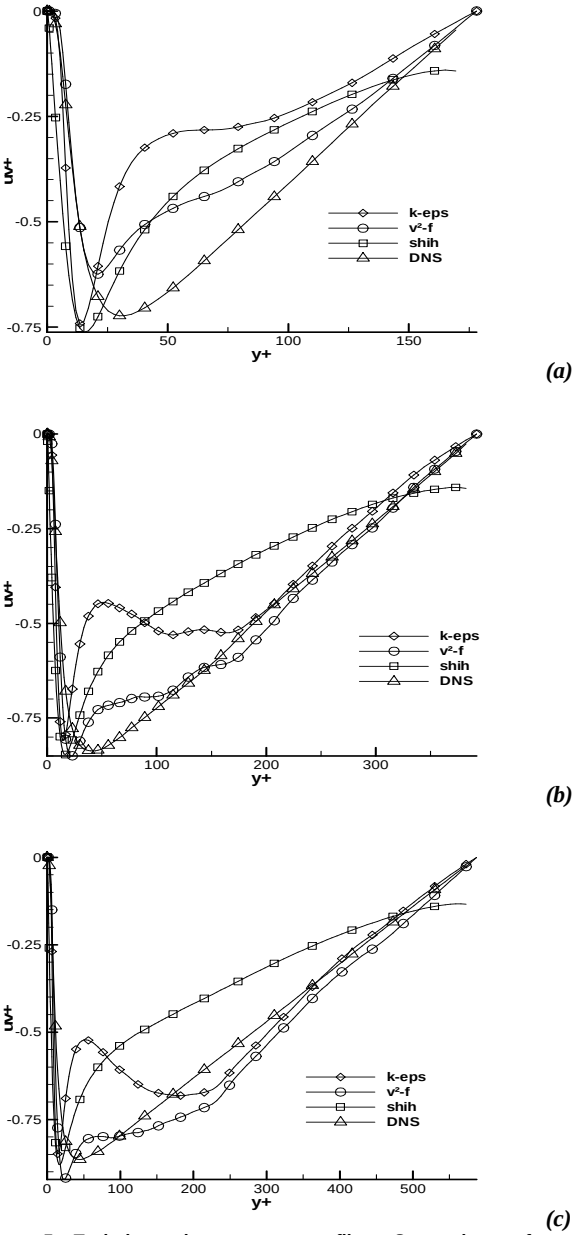


**Figure 5. Turbulent shear stress profiles. Comparison of models' predictions with DNS in a channel flow at (a)** $Re_\tau = 180$ **, (b)** $Re_\tau = 395$ **and (c)** $Re_\tau = 590$ **.**

Figure 4 depicts the prediction for the spanwise component $\overline{ww}^+$ with the three models and the DNS. The Shih model gives the better prediction when compared with the DNS, even though with an under-prediction of *50%* for the maximum value of $\overline{ww}^+$ for $Re_\tau = 590$ . In these figures (see Figs. 2, 3 and 4), we observe that the $k-\varepsilon$ and the $\overline{v^2}-f$ models give the same prediction for the three Reynolds numbers. It means that the kinetic energy is distributed in the same way for the three normal components. For these linear models, the normal components are related to the term *2k/3* as shown in Eq. (1), as for a fully developed channel flow $S_{11} = S_{22} = S_{33} = 0$ . The modeling of the eddy viscosity, using or not the component $\overline{vv}^+$ of the Reynolds stress, will not contribute to model these components. The better agreement given by the Shih model is related to the presence of non-linear terms as shown in Eq. (11).

In order to analyze the behavior of these models for the shear stress components, predictions for the three models and the DNS are shown in Fig. 5. For this component, we observe that the $\overline{v^2}-f$ gives the best agreement with the DNS results. The $k-\varepsilon$ and the Shih models under-predict this component giving an anomalous profile.

We note that the Shih model presents good agreement with the DNS data. As for the $k-\varepsilon$ and the $\overline{v^2}-f$ models, the streamwise stress component $\overline{uu}^+$ is under-predicted, while the normal stress component $\overline{vv}^+$ and the spanwise stress component $\overline{ww}^+$ are over-predicted.

Figure 5 exhibits the profiles of the normalized shear stress $\overline{uv}^+$. An analysis of this figure allows us to notice that predictions of the $\overline{v^2}-f$ model are in good agreement with the DNS results. Overall, for this component, the $k-\varepsilon$ and Shih results do not satisfactorily agree with the DNS data.

### *A posteriori* results

We call *a posteriori* test the evaluation of the results using the RANS (Reynolds Averaged Navier-Stokes) equations coupled with the turbulent model that are being tested. In this case of *a posteriori*, the results given by the numerical code, for the mean quantities concerning the velocity field and the second order moments (Reynolds stress components) and the dissipation rate are compared directly with the results of the DNS. The numerical approximation to solve the mass and the momentum conservation (Navier-Stokes equations) coupled with the turbulent models was obtained through the standard finite volume techniques on a staggered grid, where the pressure is defined at the center of very cubical grid and the velocity components at the center of every face. The normal Reynolds stresses are cell centered, while the off-diagonal terms are located at the mid-edges. A number of different upwind approximation schemes were used for representing the nonlinear terms, but no sensitivity was detected from this part of the algorithm. The solution for the equation was obtained by advancing explicitly in time the equations of motions until a steady state was reached, while enforcing the continuity at each step through the solution of the discrete Poisson equation for the pressure. Details of the algorithm can be found in Mompean and Thais (2010).

In this study, computations are achieved using the linear standard $k-\varepsilon$ and the model $\overline{v^2}-f$ turbulent model. The results are then compared with the DNS data of Moser et al. (1999). It is worth recalling that for the *a posteriori* test of the $\overline{v^2}-f$ model, the turbulent quantities are computed by solving the RANS equations in conjunction with Eqs. (1) to (10).

Figures 6, 7 and 8 depict the turbulent kinetic energy $k^+$, its dissipation rate $\varepsilon^+$, and the $\overline{uv}^+$ Reynolds tensor component respectively, for a turbulent Reynolds number of *180*. In Fig. 6, the $\overline{v^2}-f$ model is in a relatively good agreement with the DNS data, in the region near and far from the wall. The standard two-equation $k-\varepsilon$ model overestimates the level of the turbulent kinetic energy. For the dissipation rate ( $\varepsilon$ ), shown in Fig. 7, we see clearly that the corrections added to the new scales of the elliptic relaxation model improve the wall behaviour of the dissipation rate, especially near the wall. Figure 8 confirms the first results presented in the *a priori* study. The $\overline{v^2}-f$ model is in better agreement with the DNS data

than the standard $k-\varepsilon$ model, and the profile of the turbulent shear stress is relatively well predicted.

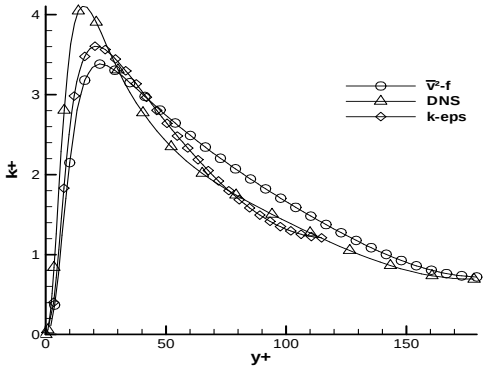


**Figure 6. Turbulent kinetic energy $k^+$ for $Re_\tau = 180$ .**

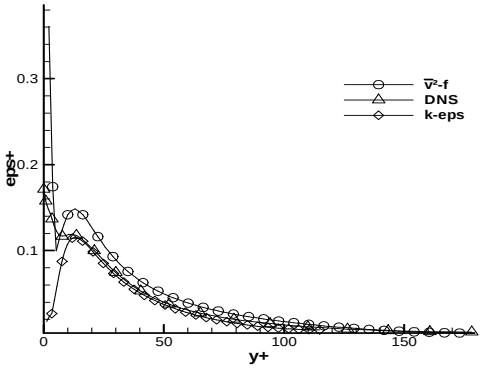


**Figure 7. Dissipation rate $\varepsilon^+$ for $Re_\tau = 180$ .**

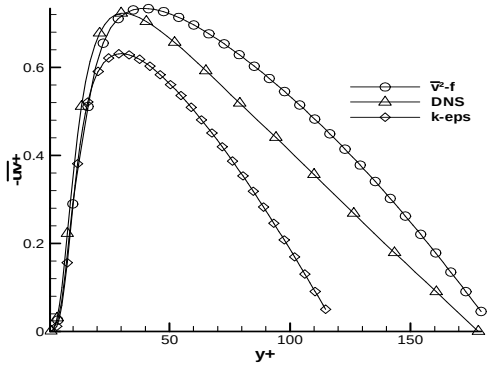


**Figure 8. Wall-shear stress component $\overline{uv}^+$ for $Re_\tau = 180$ .**

In order to generalize the results obtained, computations are performed up to Reynolds number of *590*.

In Figs. 9(a) and (b) (*log scale*), the turbulent kinetic energy and the shear stress Reynolds component are presented for a turbulent Reynolds number of *395* respectively. The $\overline{v^2}-f$ and the *k-ε* models are compared with the DNS data of Moser et al. (1999). The profile of these variables shows a noteworthy agreement between the elliptic relaxation model and the DNS data.

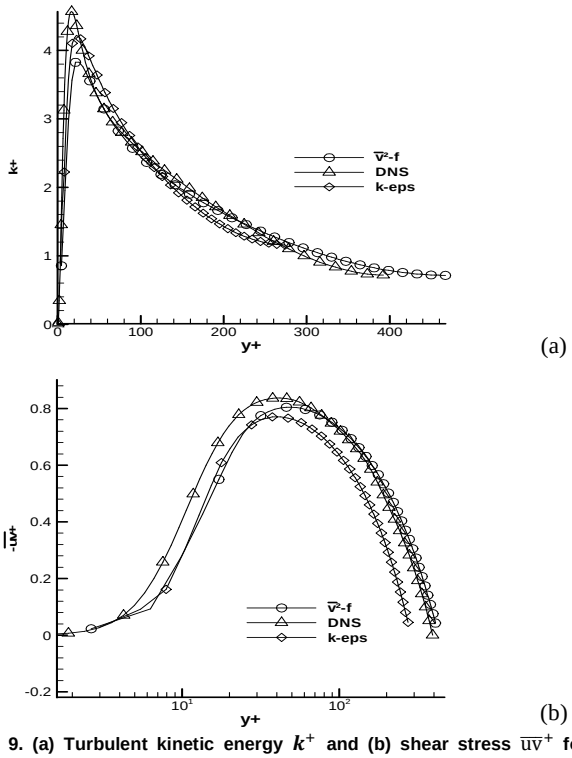


**Figure 9. (a) Turbulent kinetic energy $k^+$ and (b) shear stress $\overline{uv}^+$ for $Re_\tau = 395$ .**

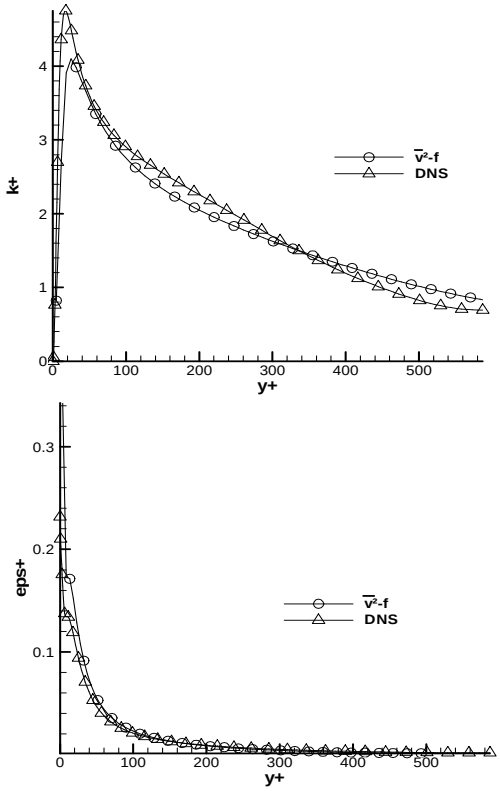


**Figure 10. Turbulent kinetic energy $k^+$ and its dissipation rate $\varepsilon^+$ for $Re_\tau$ = 590.**

As for Figs. 10 and 11, the turbulent parameters are presented for a turbulent Reynolds number of 590. In Figs. 10 and 11, the turbulent kinetic energy $k^+$ and its dissipation rate $\varepsilon^+$, and the $\overline{uv}^+$ component are presented showing a good agreement with the DNS results.

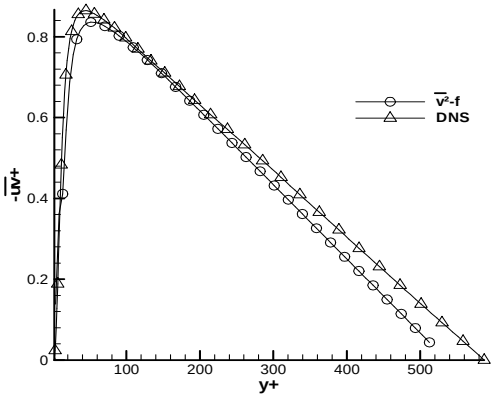


**Figure 11. Wall shear stress component $\overline{uv}^+$ for $Re_\tau$ = 590.**

## Conclusions

Linear and non-linear models of turbulence were studied using *a priori* and *a posteriori* evaluations. These models were assessed by considering the turbulent plan channel flow with a turbulent Reynolds number ( $Re_\tau = u_\tau \delta / \nu$ ) from *180* up to *590*. Comparisons with the available Direct Numerical Simulation data of Moser et al. (1999) have been presented. For the considered flow, the important points emerging from the *a priori* results are:

- The level of anisotropy between the normal stresses is well captured by the non-linear model of Shih et al. (1995).
- For the shear stress component of the Reynolds tensor, the $\overline{v^2} - f$ model gives better agreement with the DNS data for near wall turbulent flows.
- Nevertheless, the anisotropy level of the normal stresses is poorly predicted by the $\overline{v^2} - f$ model. The Shih model predicts quite correctly the level of anisotropy, but the profiles of shear stress are not in good agreement with the DNS results.

The *a posteriori* tests made with the $\overline{v^2} - f$ , have confirmed that this model is an appropriate model for flows dominated by shear, as for example the wall boundary layers. However, as expected for the *a priori* test, the $\overline{v^2} - f$ model was not able to predict correctly the level of anisotropy concerning the normal components of the Reynolds stress. This drawback of the model should be removed when using the *a posteriori* calculations, as the equation for the $\overline{vv}^+$ normal component (*y*-direction) is included in the model to predicted turbulent complex flow where the anisotropy is important. However, the question about the prediction of the right level of the streamwise (*x*-direction) and spanwise (*z*-direction) Reynolds stress components remains open. This point can be improved using non-linear terms to express the Reynolds stress and keeping the fluctuation $\overline{vv}^+$ as a turbulent scale. This topic will be considered in a future work.

## References

Chien, K.Y., 1982, "Predictions of channel and boundary layer flows with a low Reynolds number turbulence model", AIAA Journal, Vol. 20, pp. 33-38.

Durbin, P.A., 1991, "Near-wall turbulence closure modeling without damping functions", Theor. Compt. Fluid Dyn., Vol. 3, No. 1, pp. 1-13.

Durbin, P.A., 1993, "A Reynolds stress model for near-wall turbulence", Journal of Fluid Mechanics, Vol. 249, pp. 465-498.

Goldberg, U., Peroomian, O., Batten, P. and chakravarthy, S., 2009, "The $k-\varepsilon-Re_t$ turbulence closure", Engineering Applications of CFD, Vol. 3, No. 2, pp. 175-183.

Hines, J., Thompson, G.P. and Lien F.S., 2009, "A turbulent flow over a square cylinder with prescribed and autonomous motions", Engineering Applications of CFD, Vol. 3, No. 4, pp. 573-586.

Manceau, R., Carlson, J.R. and Gatski, T.B., 2002 "A rescaled elliptic relaxation approach: neutralizing the effect on the log layer", Physics of Fluids, Vol. 14, No. 11, pp.3868-3879.

Mompean, G., Gavrilakis, S., Machiels, L. and Deville, M., 1996, "On predicting the turbulence-induced secondary flows using non-linear $k-\varepsilon$ models", Physics of Fluids, Vol. 8, No. 7, pp. 1856-1868.

Mompean, G. and Thais, L., 2010, "Finite Volume Simulation of Viscoelastic Flows in General Orthogonal Coordinates", Mathematics and Computers in Simulation, Vol. 80, pp. 2185-2199.

Moosavi, R. and Grandjalikhan Nassab, S.A., 2008, "Turbulent forced convection over a single inclined forward step in a duct: Part I - flow field", Engineering Applications of CFD, Vol. 2, No. 3, pp. 366-374.

Moser, R.D., Kim, J. and Mansour, N.N., 1999, "Direct numerical simulation of turbulent channel flow up to Re=590", Physics of Fluids, Vol. 11, No. 4, pp. 943-945.

Naji H., Mompean, G. and El Yahyaoui, O., 2004, "Evaluation of explicit algebraic stress models using direct numerical simulations", Journal of Turbulence, Vol. 5, No. 38, pp. 1-25.

Qiu, X., Mompean, G., Schmitt F. and Thompson, R.L., 2011, "Modeling turbulent flow using viscoelastic viscometric functions", Journal of Turbulence. Vol. 12, No. 15, pp.1-18.

Shih, T.H., Zhu, J. and Lumley, J., 1995, "A new Reynolds stress algebraic equation model", Comp. Meth. Appl. Mech. Eng., Vol. 125, No. 1, pp. 287-302.

Thompson, R.L., Mompean, G. and Thais, L., 2010, "A methodology to quantify the non-linearity of the Reynolds stress tensor", Journal of Turbulence, Vol. 11, No. 33, pp.1-27.